Pb 4f photoelectron spectroscopy on mass-selected anionic lead clusters at FLASH

2012 New J. Phys. 14 075008

(http://iopscience.iop.org/1367-2630/14/7/075008)

New Journal of Physics
The open-access journal for physics

Pb 4f photoelectron spectroscopy on mass-selected anionic lead clusters at FLASH

J Bahn[1,8], P Oelßner[1,8], M Köther[1,8], C Braun[2], V Senz[1], S Palutke[3], M Martins[3], E Rühl[4], G Ganteför[2], T Möller[5], B von Issendorff[6], D Bauer[1], J Tiggesbäumker[1] and K-H Meiwes-Broer[1,7]

[1] Department of Physics, University of Rostock, Universitätsplatz 3, D-18055 Rostock, Germany
[2] Department of Physics, University of Konstanz, Universitätsstraße 10, D-78464 Konstanz, Germany
[3] Department of Physics, University of Hamburg, Luruper Chaussee 149, 22761 Hamburg, Germany
[4] Department of Physics, Free University of Berlin, Arnimallee 14, D-14195 Berlin, Germany
[5] Department of Physics, Technical University of Berlin, Hardenbergstr. 36, 10623 Berlin, Germany
[6] Department of Physics, University of Freiburg, Hermann-Herder-Str. 3a, D-79104 Freiburg, Germany
E-mail: meiwes@uni-rostock.de

New Journal of Physics **14** (2012) 075008 (10pp)
Received 27 February 2012
Published 3 July 2012
Online at http://www.njp.org/
doi:10.1088/1367-2630/14/7/075008

Abstract. 4f core level photoelectron spectroscopy has been performed on negatively charged lead clusters, in the size range of 10–90 atoms. We deploy 4.7 nm radiation from the free-electron laser FLASH, yielding sufficiently high photon flux to investigate mass-selected systems in a beam. A new photoelectron detection system based on a hemispherical spectrometer and a time-resolving delayline detector makes it possible to assign electron signals to each micro-pulse of FLASH. The resulting 4f binding energies show good agreement with the metallic sphere model, giving evidence for a fast screening of the 4f core holes. By comparing the present work with previous 5d and valence region data,

[7] Author to whom any correspondence should be addressed.
[8] J Bahn, P Oelßner and M Köther equally contributed to this work.

the paper presents a comprehensive overview of the energetics of lead clusters, from atoms to bulk. Special care is taken to discuss the differences of the valence- and core-level anion cluster photoionizations. Whereas in the valence case the escaping photoelectron interacts with a neutral system near its ground state, core-level ionization leads to transiently highly excited neutral clusters. Thus, the photoelectron signal might carry information on the relaxation dynamics.

Contents

1. Introduction

The properties of metal clusters and nanoparticles with defined numbers of atoms N can show a fascinating N-dependent evolution, from atoms to bulk. Such studies have already led to far-reaching insight into the nature of finite-sized matter [1]. The most direct method to investigate the electronic level structure is photoelectron spectroscopy (PES). PES on clusters has a long history, comprising systems grown at surfaces [2, 3], deposited from beams [4–7] and in gas phase. The latter yielded a fundamental understanding of how the electronic structure develops when the number of atoms N changes. By using UV lasers, details of valence shells are accessible as well as threshold energies [8–15]. The accompanying density functional and other quantum chemical calculations helped us to resolve the transition from atoms to bulk [15, 16].

Concerning inner-shell photoemission on isolated systems prepared in molecular beams, only a few studies have been conducted so far. This is surprising at first, since astounding effects are expected in the core-level regime. Among those are the N dependence of the level positions, Auger and possibly inter-atomic Coulomb decay processes [17]. Further relaxation pathways might appear as signatures in the photoelectron spectra, such as shake-up, shake-off and shake-down [18]. The involved phenomena touch fundamental questions of many-particle physics. In particular, when dealing with metal clusters strong electronic correlations might govern photoionization. Already the inner-shell ionization of atoms and the subsequent decay mechanisms are a topical issue. For example, in the case of neon, a strong interplay between outer-valence, inner-valence and core–shell processes could theoretically be disentangled [19]. Recent experimental studies at the x-ray free-electron laser LCLS demonstrated that rapid sequential excitations lead to multiple inner-shell vacancy formation and thus the creation of hollow Ne atoms [20].

In rare gas clusters, the electronic structure has been probed with soft x-rays, revealing core excited excitons [21–23] as well as surface and bulk states [24–26]. Shifts in core ionization energies have been assigned in terms of polarization screening [27]. Work on metal clusters exhibits core-level and Auger signatures which served, e.g., to determine the cluster size [28–30]. However, these investigations suffer from the lack of any clear size dependence,

since only cluster size distributions that are formed in jet expansions could be studied. In the present work, on the other hand, mass-selected cluster anions Pb_N^- are prepared. Similar to previous studies [31] the cluster is neutral after ionization but transiently in a highly excited state, which will trigger strong relaxation dynamics, potentially influencing the interaction of the departing photoelectron with the residual cluster. We could show that for $N \geqslant 20$ the size-dependent change of the 5d binding energies follows the metallic sphere model, thus hinting at perfect screening of the core hole. Deviations for smaller N have been interpreted as an indication of a change in the bonding character, i.e. a metal to non-metal transition around $N \simeq 20$. These data enter figure 4 for comparison. DFT studies have strengthened the interpretation of this transition as a metal to non-metal one [16].

The experimental challenge in inner-shell PES on *mass-selected* clusters lies in the notoriously dilute target densities. Therefore, synchrotron studies are limited to unselected neutrals, see above, or for x-ray absorption studies on ions stored in a trap [32]. With the now decreased photon wavelength of FLASH down to 5 nm, deeper core levels become accessible. In the present study on Pb_N^-, we report on 4f PES, exhibiting a size-dependent core-level shift. One question is whether the 4f levels follow the metallic sphere model, which predicts the behavior of the ionization potential and the electron detachment energy (E_D) of metallic spheres in relation to their radius [33–35]. For clusters, the radius can be approximated by $R(N) = N^{1/3} r_s + a_0$, with r_s being the Wigner–Seitz radius of lead (1934 Å, as estimated from bulk density), and the Bohr radius a_0 to account for the electron spill-out. We are aware of the fact that the concept of electron spill-out is not the best to describe changes in the cluster radius. However, currently this approximation may serve to account for the slightly decreasing atom density in small lead clusters when compared to bulk. Extending this model to inner-shell ionization of negatively charged metallic clusters, hence assuming full screening of the core hole, leads to the following expression for the N dependence of the 4f 'detachment' energies:

$$E_D(R) = WF_{bulk} + E_{4f} - \frac{1}{2} \frac{e^2}{4\pi\varepsilon_0 R(N)},$$

with WF_{bulk} being the bulk work function and E_{4f} the bulk 4f energy relative to the Fermi level. In a $1/R$ plot the expression gives straight lines; see figure 4.

The paper is organized as follows: the experimental section gives details of the cluster beam setup and of the new photoelectron detection system, adapted to the pulse timing at free-electron lasers such as FLASH. Next the 4f binding energies as obtained by the new system will be compared to the metal sphere model. The following discussion includes previous 5d and valence PES data of lead clusters, giving rise to a more in-depth consideration of the ionization dynamics.

2. The experimental setup

A laser vaporization source [8, 36] serves to produce negatively charged lead clusters. The particles are accelerated with a 1 kV pulsed electric field and the beam formation is controlled with ion optics. For mass separation a time-of-flight mass spectrometer is used where the clusters are detected with a channeltron just after the interaction zone with the FLASH beam; see figure 1. As helium is pumped into the source for cluster formation, maintaining the huge pressure gradient from several mbar in the source to 10^{-10} mbar during photoionization is a significant challenge. Intense light pulse trains at a photon energy of 263.5 eV (4.7 nm

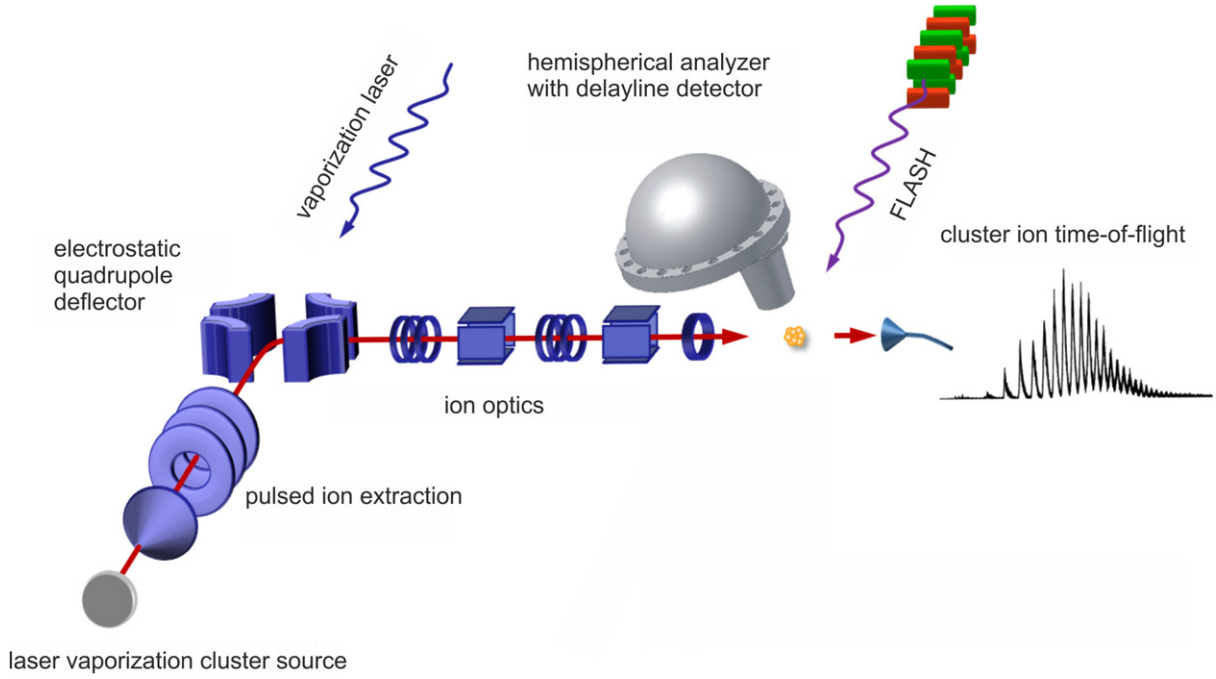

Figure 1. Schematic view of the experimental setup for conducting soft x-ray PES on mass-selected clusters. The cluster beam is produced by a pulsed laser vaporization source. After acceleration with a 1 kV electric field the clusters are guided and focused into the interaction region. There, the mass-resolved cluster bunches overlap with radiation from FLASH. A hemispherical analyzer with a maximum detection angle of $\pm 13^{\circ}$ disperses the electrons which are registered in a delayline detector allowing for time-resolved electron detection. Due to the separation in time it is possible to assign the electron signals to the corresponding cluster sizes.

wavelength) are supplied by the FLASH beam line 1 (BL1). This train contains up to 200 micro-pulses, which are separated by 1 μs. As the repetition rate of FLASH is 10 Hz, the rate of the experiment is set to the same value. The interaction zone is deliberately placed 1.5 m out of the FLASH focal point in order to reduce the peak intensity and illuminate a 1.5 mm spot, which matches the size of the cluster beam. By this a sufficiently large number of clusters is exposed and multi-photon effects can largely be neglected.

Much attention has to be given to the photoelectron spectrometer design, as it realizes a big advancement for the experimental setup. The magnetic-bottle-type time-of-flight electron spectrometer which was employed in previous experiments at FLASH suffered from saturation by the high signal load due to electrons from the source operation gases and background electrons. Due to these limitations this system has been replaced by a hemispherical analyzer combined with a transfer lens system (SPECS PHOIBOS 150). It is mounted under the magic angle of 54.7°. The analyzer is equipped with a two-dimensional delay-line detector, which enables the system to measure angular resolved kinetic energy spectra. However, the instrument can be operated in the wide-angle mode to spatially collect as many electrons as possible. With about 50 μJ in each micro-pulse, 10^{12} photons are available to excite about 500 clusters in a

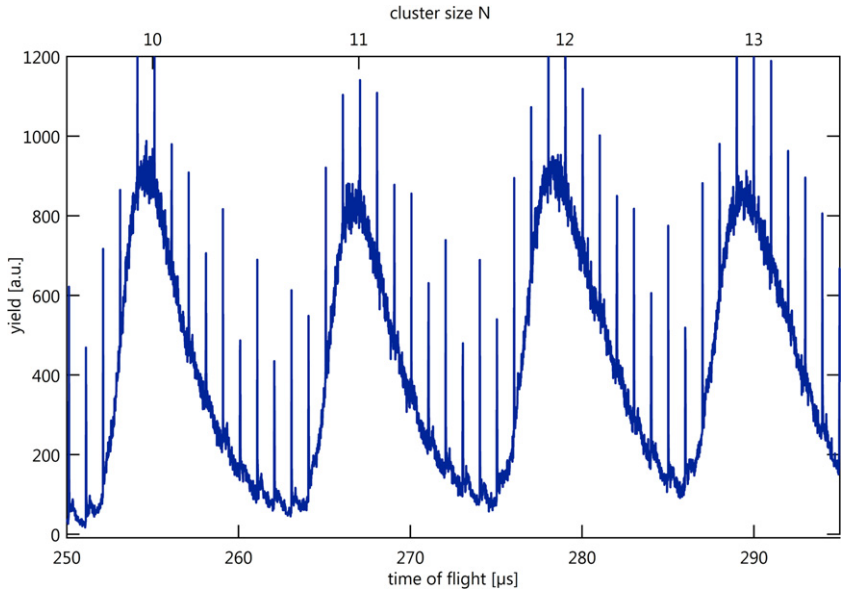

Figure 2. Timing control of cluster mass peaks (broad features) and the FLASH micro-pulses (narrow features on top of the mass peaks). The channeltron detector registers the cluster ions simultaneously with stray light from FLASH. With the gated electron spectrometer photoelectrons from each single micro-pulse are selectively registered.

volume of 1.5 mm diameter and 5 mm length. Assuming the atomic 4f cross section of 2.14 Mbarn and an electron collection efficiency of 1%, we arrive at a rate of about 0.5 count per micro-pulse and cycle.

As the ion acceleration and the delay-line detector are triggered by the FLASH pulsing system, the pulse train overlaps in time with a defined cluster size range [31]. Thus photoelectrons released by each micro-pulse can be assigned to a given cluster size. Figure 2 shows a section of the mass spectrum with additional signatures of FLASH. The ions as well as the FLASH stray light signals are registered simultaneously by the channeltron. With this method only a few delay settings are necessary to record PES of a wide range of selected clusters, in our experiment $\Delta N = 10$–90. Figure 3 displays examples of photoelectron spectra corresponding to $N = 40$–62, each obtained by summarizing the signals of 20 micro-pulses.

3. Results and discussion

For the analysis of spectra like in figure 3, the exact photon energy of each FLASH micro-pulse has to be known. In fact, previous studies and current PES measurements of different rare gases have shown that there might be smooth shifts in photon energy over the entire micro-pulse train, of the order of eV. Thus, a corresponding correction is mandatory. We chose the 3d PES from krypton and checked it against the estimated 4f location of lead clusters with $N \simeq 80$, as well as against the spin–orbit splitting of the Pb 4f levels. Next, photoelectron signals from micro-pulses hitting the same cluster size can be accumulated and fitted. Figure 4 (top) shows the extracted 4f binding energies for both spin–orbit components. The energy scale is referenced to

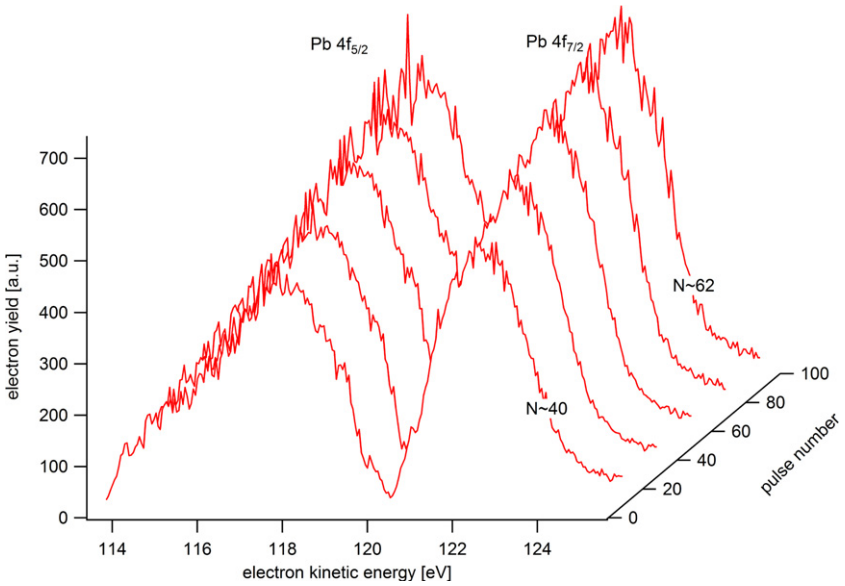

Figure 3. Set of photoelectron spectra from selected clusters with given sizes, obtained with a fraction of the FLASH pulse train. All spectra are obtained simultaneously with the same delay setting.

the vacuum energy, in order to allow for a direct comparison to the metal sphere model, which appears as straight lines in a $1/R$ plot, like in figure 4. Within the error limits the experimental data generally follow the model, which is pinned to measured bulk 4f core level energies plus WF_{bulk}. We may note that for WF_{bulk} of lead two values can be found in the literature, one obtained by photoelectric measurements [39] and one by extrapolation of PES from unselected clusters [29]. For the lines in figure 4 the bulk result is used, depicted by the top edges of the boxes at the left scale. Extrapolation towards the atom reaches values which are about 1 eV above the corresponding measurements. Table 1 compiles the different bulk and atomic energies involved in figure 4. For clusters with N below 20 both 4f spin–orbit components show a slight tendency to deviate from the model and drop below the estimated binding energy.

In addition to the current results, figure 4 summarizes previously obtained 5d binding energies as well as valence photodetachment energies of Pb_N^-. All the data show absolute values and N dependences roughly in accordance with the classical metal sphere model. As usually in PES, with increasing electron energy the experimental resolution decreases. In the experimental run, presented here, a resolution in the range of 2% is achieved, with the FLASH bandwidth being the by far limiting factor for the precision of the 4f data.

When comparing the core-level results to valence detachment energies (bottom of figure 4), one should remember that the latter specify anion photoemission thresholds, which usually differ from peak centroids. In particular the valence PES of Pb_N^- are characterized by partially well-resolved narrow peaks which may cover a 2 eV range of the spectrum [9, 38]. Moreover, in one case the authors define the first narrow peak as the electron detachment energy, and in the other case the onset of electron intensity is chosen. Thus there appear slight differences in the valence data, although the measured spectra might completely coincide. Beyond $N \simeq 25$, however, the peaked spectra disappear and are replaced by more smooth intensity onsets. Interestingly, this is the size range below which the core-level data show a more or less

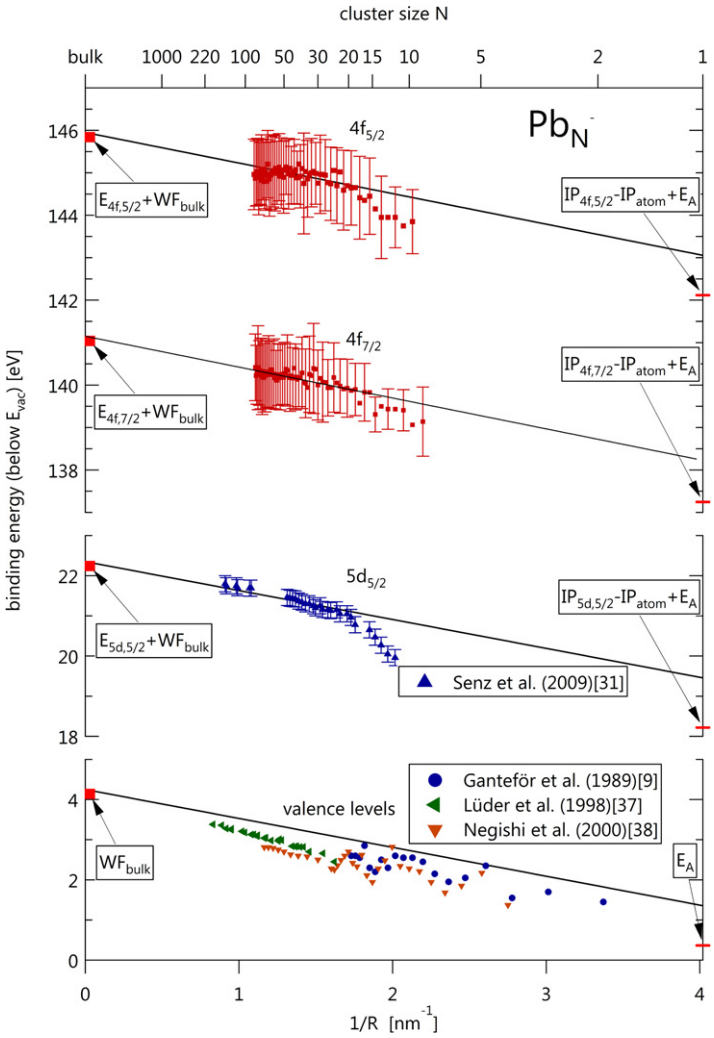

Figure 4. Binding energies E_{D} of negatively charged lead clusters *versus* the inverse cluster radius $1/R$. The straight lines result from the metallic sphere model; see text. On the left axis the bulk binding energies are shown. The values on the right axis are derived from the atomic electron affinity and ionization potentials. See table 1 for the corresponding sources [9, 37, 38].

pronounced deviation from the metal sphere model. As pointed out above, the deviation, first observed for the 5d levels, was rationalized through a not fully screened core hole [31]. So far this *ad-hoc* model has not yet been backed by a thorough theoretical consideration. In the current Focus Issue of *New Journal of Physics*, an *all-electron atom in jellium* model for the study of core–shell ionization is introduced [40].

The results in figure 4 might suggest that the deviation from the spherical model is weaker for the 4f when compared to the 5d levels. One reason could be the different photon energies that have been employed in the two experiments, leading to different kinetic energies of $\simeq 120$ and $\simeq 15$ eV in the 4f- and 5d cases, respectively. It is known that if the photoelectron escapes rapidly, a part of the relaxation energy does not go to the photoelectron but remains

Table 1. Energies as used in figure 4 for the bulk and atomic limits of lead, in eV. Note that all the data rely on experimental work.

Bulk work function	Bulk binding energies relative to E_F			Electron affinity	Atomic ionization potential	Atomic core-level ionization energies		
WF_{bulk}	$E_{5d,5/2}$	$E_{4f,7/2}$	$E_{4f,5/2}$	E_A	IP_{atom}	$IP_{5d,5/2}$	$IP_{4f,7/2}$	$IP_{4f,5/2}$
4.0–4.25 [29, 39]	18.1 [41]	136.9 [42]	141.7 [42]	0.365 [43]	7.417 [44]	25.27 [45]	144.3 [46]	149.17 [46]

as excitation in the residual system. In fact, in the high-photon-energy limit the photoelectron spectrum should be centered around the Hartree–Fock energy [47, 48], which, according to Koopmans' theorem, is the binding energy evaluated with the *unrelaxed* final-state energy. As a consequence, the absolute value of the binding energy inferred from the photoelectron peak should increase if the photoelectron 'has no time' to pick up the relaxation energy. The time the photoelectron spends inside a 30-atom cluster is estimated from the above kinetic energies to be $\simeq 100$ as and $\simeq 300$ as in the 4f- and 5d cases, respectively.

The screening dynamics of core-holes depend on the level scheme but may be separated at least into two time scales, namely the faster one due to the other electrons in the same atomic subshell and a slower one due to the valence electrons. The theoretical work [40], albeit considering 2p-emission from Na clusters, suggests that the latter time scale is already on a sub-fs level. The former inner-atomic relaxation of the 2p occurs within tens of attoseconds. Hence, only for smaller clusters or significant higher photon energies the valence-electron screening may be comparable to or even slower than the escape times. Consequently, electrons with different escape times might probe different relaxation states, an interesting subject for future studies on electron correlation phenomena. For a more complete picture one should also consider (inneratomic) Auger-like relaxation, which occurs within femtoseconds (2.3 fs for Pb [49]). In fact, if the Auger relaxation energy went to the photoelectron, its peak would indicate a *much* lower binding energy. Instead, the Auger relaxation energy is mainly distributed over valence electrons, giving rise to broad inelastic features in the spectra [50], generated after the primary photoelectron escaped. Indeed, all our core-level spectra go along with strong emission of low-energy electrons, a subject that has to be dealt with in the future. The valence photoelectron spectra, on the other hand, usually do not show significant low-energy intensity.

The observed deviation from the metal sphere model could also be due to initial state effects, i.e. electronic structure. A possible explanation could be based on a size-dependent contraction of the 6s orbitals. In lead the atomic 6s orbital is contracted and strongly bound due to relativistic effects, making lead predominantly divalent [51]. This localization might be increasingly important in small systems, where larger bond lengths have been predicted [16]. Softer bonds lead to smaller overlaps of the 6s orbitals, yielding a reduced electron delocalization. The resulting enhancement of the 6s electron localization could cause the observed binding energy reduction of the core levels below the metal sphere result. This also explains the stronger effect for the 5d levels, which are spatially more extended than the 4f levels and therefore more susceptible to changes in the 6s orbital extension.

4. Conclusion

Soft x-ray photoemission on mass-selected lead cluster anions using 4.7 nm light pulses delivered by FLASH shows a size-dependent change in the 4f binding energies beyond Pb_{20}, indicating a full screening of the core hole. Deviations from the metal sphere model for smaller systems are in qualitative agreement with previous results obtained for the 5d levels and hint at a change in the bond character from a metallic to a non-metallic cluster. The different slopes for 4f and 5d below $N = 20$ suggest that the photoelectron probes different time scales of the relaxation energetics. This might pave the way for resolving the relaxation dynamics in size-selected clusters in future studies.

Acknowledgments

We gratefully acknowledge experimental support from the FLASH team and from A Oelsner of Surface Concept (GmbH). This work was funded by the BMBF, FSP 301—FLASH under contracts 05KS7KT1 and 05KS7HR1 and by the Collaborative Research Center SFB 652 at the University of Rostock.

References

[1] Sattler K D (ed) 2010 *Handbook of Nanophysics: Clusters and Fullerenes* (Boca Raton, FL: CRC Press)
[2] Wertheim G K, DiCenzo S B and Buchanan D N E 1986 *Phys. Rev.* B **33** 5384
[3] Bromann K, Brune H, Giovannini M and Kern K 1998 *Nature* **394** 451
[4] Eberhardt W, Fayet P, Cox D M, Fu Z, Kaldor A, Sherwood R and Sondericker D 1990 *Phys. Rev. Lett.* **64** 780
[5] Siekmann H R, Holub-Krappe E, Wrenger B, Pettenkofer Ch and Meiwes-Broer K H 1993 *Z. Phys.* B **90** 201
[6] Wertheim G K 1989 *Z. Phys.* D **12** 319
[7] Balkaya B, Ferretti N, Neeb M, Peters S, Peredkov S and Eberhardt W 2010 *Phys. Chem. Chem. Phys.* **12** 9867
[8] Taylor K J, Pettiette-Hall C L, Cheshnovsky O and Smalley R E 1992 *J. Chem. Phys.* **96** 3319
[9] Ganteför G, Gausa M, Meiwes-Broer K-H and Lutz H O 1989 *Z. Phys.* D **12** 405
[10] Leopold D G, Ho J and Lineberger W C 1987 *J. Chem. Phys.* **86** 1715
[11] Ganteför G, Meiwes-Broer K H and Lutz H O 1988 *Phys. Rev.* A **37** 2716
[12] Lee G H, Sarkas H W, Kidder L H, Snodgrass J T, Manaa M R, McHugh K M, Eaton J G and Bowen K H 1989 *J. Chem. Phys.* **91** 3792
[13] Möller H, Cha C-Y, Bechthold P S, Ganteför G, Handschuh H and Eberhardt W 1996 *Surf. Rev. Lett.* **3** 399
[14] Wrigge G, Astruc Hoffmann M and von Issendorff B 2002 *Phys. Rev.* A **65** 063201
[15] Kostko O, Huber B, Moseler M and von Issendorff B 2007 *Phys. Rev. Lett.* **98** 043401
[16] Wang B, Zhao J, Chen X, Shi D and Wang G 2005 *Phys. Rev.* A **71** 033201
[17] Hergenhahn U, Marburger S, Kugeler O and Möller T 2003 *Phys. Rev. Lett.* **90** 203401
[18] Randal K J, Feldhaus J, Kilcoyne A L D, Bradshaw A M, Xu Z, Johnson P D, Eberhardt W, Rubensson J-E and Ma Y 1992 *Phys. Scr.* **T41** 143
[19] Rohringer N and Santra R 2007 *Phys. Rev.* A **76** 033416
[20] Krässig B *et al* 2010 *Nature Phys.* **466** 56
[21] Hitchcock A P, Rühl E, Heinzel C and Baumgärtel H 1993 *J. Chem. Phys.* **98** 2653
[22] Wassermann B, Knop A and Rühl E 1998 *Phys. Rev. Lett.* **80** 2302
[23] Beutler A, Federmann F, Björneholm O and Möller T 1994 *Phys. Rev. Lett.* **73** 1549
[24] Björneholm O, Federmann F, Fössing F and Möller T 1995 *Phys. Rev. Lett.* **74** 3017

[25] Tchaplyguine M, Feifel R, Marinho R R T, Gisselbrecht M, Sorensen S L, Naves de Brito A, Mårtensson N, Svensson S and Björneholm O 2003 *Chem. Phys.* **289** 3
[26] Hatsui T, Setoyama H, Kosugi N, Wassermann B, Bradeanu I L and Rühl E 2005 *J. Chem. Phys.* **15** 154304
[27] Fössing F, Möller T, Björneholm O, Federmann F and Stampfli P 1996 *J. Chem. Phys.* **104** 1846
[28] Peredkov S *et al* 2007 *Phys. Rev.* B **75** 235407
[29] Peredkov S *et al* 2007 *Phys. Rev.* B **76** 081402
[30] Tchaplyguine M *et al* 2007 *Eur. Phys. J.* D **45** 295
[31] Senz V *et al* 2009 *Phys. Rev. Lett.* **102** 138303
[32] Lau J T, Rittmann J, Zamudio-Bayer V, Vogel M, Hirsch K, Klar Ph, Lofink F, Möller T and von Issendorff B 2008 *Phys. Rev. Lett.* **101** 153401
[33] Perdew J P 1988 *Phys. Rev.* B **37** 6175
[34] Seidl M and Perdew J P 1994 *Phys. Rev.* B **50** 5744
[35] Seidl M and Brack M 1996 *Ann. Phys.* **245** 275
[36] Heiz U, Vanolli F, Trento L and Schneider W-D 1997 *Rev. Sci. Instrum.* **68** 1986
[37] Lüder Ch. and Meiwes-Broer K-H 1998 *Chem. Phys. Lett.* **294** 391
[38] Negishi Y, Kawamata H, Nakajima A and Kaya K 2000 *J. Electron Spectrosc. Relat. Phenom.* **106** 117
[39] Michaelson H B 1977 *J. Appl. Phys.* **48** 4729
[40] Bauer D 2012 *New J. Phys.* **14** 055012
[41] Liu F Q, Ibrahim K, Lai W Y, Xu M C, Qian H J and Wu S C 2001 *Solid State Commun.* **117** 327
[42] Fuggle J C and Mårtensson N 1980 *J. Electron Spectrosc. Relat. Phenom.* **21** 275
[43] Feigerle C S, Corderman R R and Lineberger W C 1981 *J. Chem. Phys.* **74** 1513
[44] Johansson B and Mårtensson N 1980 *Phys. Rev.* B **21** 4427
[45] Sandner N, Schmidt V, Mehlhorn W, Wuilleumeir F, Adam M Y and Desclaux J P 1980 *J. Phys. B: At. Mol. Opt. Phys.* **13** 2937
[46] Kantia T, Heinäsmäki S, Aksela S, Patanen M, Urpelainen S and Aksela H 2011 *Phys. Rev.* A **83** 053408
[47] Manne R and Åberg T 1970 *Chem. Phys. Lett.* **7** 282
[48] Lundqvist B 1969 *J. Phys.: Condens. Matter* **9** 236
[49] Urpelainen S, Kantia T, Heinäsmäki S, Patanen M, Aksela S and Aksela H 2011 *J. Electron Spectrosc. Relat. Phenom.* **183** 59
[50] Egelhoff W F 1987 *Surf. Sci. Rep.* **6** 253
[51] Larsson P, Pyykkö P, Ahuja R, Blomqvist A and Zaleski-Ejgierd P 2011 *Phys. Rev. Lett.* **106** 018301